Deuterium retention in tin (Sn) and lithium–tin (Li–Sn) samples exposed to ISTTOK plasmas

J.P.S. Loureiro [a,*], H. Fernandes [a], F.L. Tabarés [b], G. Mazzitelli [c], C. Silva [a], R. Gomes [a], E. Alves [a], R. Mateus [a], T. Pereira [a], H. Figueiredo [a], H. Alves [a]

[a] *Instituto de Plasmas e Fusão Nuclear, Instituto Superior Técnico, Universidade de Lisboa, 1049-001 Lisboa, Portugal*
[b] *Laboratorio Nacional de Fusion, Ciemat, Avenida Complutense 22, E-28040 Madrid, Spain*
[c] *ENEA, C.R. Frascati, Via E. Fermi 45,00044 Frascati, Roma, Italy*

ABSTRACT

The use of lithium (Li) or tin (Sn) as a liquid metal plasma facing component is proposed as a solution to the high power load issue on the divertor region of nuclear fusion reactors. The possibility to use these materials depends on their compatibility with hydrogen plasmas. With the purpose of realizing deuterium retention studies, specimens of pure Sn (99.999% Sn) and Li–Sn alloy (30 at.% Li) were exposed in the ISTTOK edge plasma. *Ex situ* analysis of the samples was performed by means of ion beam diagnostics. Nuclear reaction analysis (NRA) technique was applied using the $D(^3He,p)^4He$ reaction to quantify the fuel retention on the samples.

In this work the deuterium retention is compared between pure Sn and Li–Sn alloy samples in both liquid and solid states. All the samples were found to have retention ratios smaller than 0.1 at.%. This low retention ratio is expected for pure tin given its high mass and the instability of tin hydrides. However the retention was unexpectedly low for the case of Li–Sn which was thought to be dominated by the lithium fraction in the alloy. These results suggest that tin has a role in the retention mechanism in this material.

1. Introduction

The use of liquid metals (LM) as materials in plasma-facing components (PFC) has been proposed as a possible alternative to the solid PFC in order to cope with the high power loads impinging on the first wall and particularly the divertor region of fusion reactors. The regenerative properties of the liquid surface and "vapour shielding" effect are part of the advantages that come from using a liquid wall. Metals such as lithium (Li) [1], gallium (Ga) [2] or tin (Sn) [3] have been suggested as well as the lithium–tin (Li–Sn) alloy (30 at.% Li) which is expected to display the beneficial properties of both its constituent elements [4]. The application of these materials in fusion reactors depends on their compatibility with the plasma. The discharge degradation induced by the enhanced

impurity contamination and their affinity to retain hydrogenic isotopes are two important factors.

In the framework of liquid metal PFC the most commonly used material in the literature is lithium [1,5,6] where it has been used in several configurations and different magnetic confinement fusion devices due to its low atomic mass. However lithium's evaporation rate quickly becomes a problem as temperatures increases thus limiting its utilization. The other two elements, gallium and tin, are not so commonly used. Previously, studies were performed in ISTTOK with gallium to understand its behavior in tokamak conditions [2,7]. Therefore working with tin was deemed relevant and the results regarding deuterium retention will be discussed here. The work with Li–Sn alloy is also discussed here as its hybrid behavior of both low and high nuclear mass materials revealed unpredictable results.

In this work we aim at an evaluation of the deuterium retention in two materials: pure Sn and Li–Sn alloy each exposed in two states, liquid and solid. The total integrated exposure time was kept close for all samples so that their respective retention is comparable. With this intent the samples were exposed to the edge

plasmas of the tokamak ISTTOK for several of its alternated current (AC) discharges [8,9]. Fixed radial position and similar plasma conditions were used for each sample exposure. Deuterium retention measurements were achieved by means of ion beam analysis.

2. Experimental setup

Recently, an experimental setup has been developed to produce and expose LM samples in both liquid and solid states to ISTTOK plasmas which has been described in greater detail in [10] and built upon the previously used systems described in earlier work with gallium [7]. It consists of two assemblies: a manipulator and an auxiliary controlled preparation chamber. The manipulator is a system that allows the vertical positioning of the sample. It includes the sample holder head which has an embedded electrical cartridge heater granting it its heating capabilities (required to melt the samples). The sample is placed on top of the holder head which has a cylindrical cavity with an internal radius of 5 mm, external radius of 6 mm and a depth of 2 mm. This manipulator is either installed in the auxiliary chamber, during sample preparation, or in the tokamak, for sample exposure. The auxiliary chamber offers more control and accessibility during the preparation of the samples while mimicking the ultra high vacuum (UHV) conditions of the tokamak vessel. It has a window which allows for the visual inspection of the sample preparation as well as an horizontal manipulator (perpendicular to the main one).

2.1. Sample preparation

The Sn used in this work is a 99.999% pure rod sourced from MaTeck [11] (Lot. No. 14011517) and the Li–Sn alloy was produced by alloying pure Li and Sn metals under vacuum at the Nuclear Radiations Laboratory at the U. Illinois Urbana. Its composition was chosen to be 30 at.% lithium and 70 at.% tin ($Li_{30}Sn_{70}$).

First, to assure a good wetability of holder's cup it was necessary to have the stainless steel substrate cleaned in hydrochloric acid followed by a ultrasonic bath. Good wetting of the metallic sample to the holder is necessary since there is no porous system holding the sample.

The sample was placed in the cleaned holder and the full manipulator was installed in the auxiliary chamber. The main purpose of this chamber is to monitor the first heating and consequent melting of the sample material under UHV. The current in the electrical heater is raised until the surface temperature of the sample is above melting point. Then these conditions are kept until the sample is uniformly molten and the pressure becomes stable. It is common to observe a migration of impurities (mostly metal dross) to the liquid surface during this period. When this occurs the horizontal manipulator is used to rasp the surface. This is of particular importance to the Li–Sn alloy since minimal exposure to the atmosphere can lead to oxidation which is known to alter the properties of the surface exposed to the plasma. Following this procedure the sample has an exposed circular area of 78.5 mm^2 and 2 mm of material protruding from the holder. Fig. 1 depicts a Sn sample in the holder. After the preparation in the auxiliary chamber the manipulator assembly (which contains the sample) is quickly transferred to the tokamak.

Once there the sample is again degassed, lifted to the selected height for exposure and reheated. When installed in the tokamak the surface temperature of the samples can be monitored using a pyrometer (optris CTlaser 3ML) focused on the sample from the top connector of the port.

Fig. 1. Tin sample in its holder after exposure to ISTTOK plasmas.

2.2. Sample exposure in ISTTOK

The samples were exposed in ISTTOK, a high aspect ratio tokamak with a circular cross-section. Its main parameters are: $R = 46$ cm, $a = 8.5$ cm, $B_T = 0.5$ T, $I_p = 5$ kA. One of the main advantages of this device is the fact that it can be operated in AC-mode [8], meaning that each discharge consists of several alternated pulses, which was made possible due to improvements in the real-time control system of ISTTOK [9,12]. This operation mode extends the length of discharge decreasing the time it takes to attain the desired sample exposure. The available parameters in the edge plasma, where the samples are exposed, are: electron and ion temperature, $T_e \sim T_i = 20 - 40$ eV, electron density, $n_e = 0.5 - 3 \times 10^{18}$ m^{-3}, particle flux $\Gamma^{D+} = 1 - 7 \times 10^{22}$/m^{2}s, a radial decay length of the particle flux of $\sim 2 - 3$ cm and discharge duration of 250 ms (with each shot consisting of ten alternating pulses with a duration of ~ 25 ms).

The manipulator was inserted from a lower vertical port of the tokamak with the sample exposition surface kept parallel to the machine horizontal plane. Samples were exposed at a normalized radial position of $r/a = 0.8$, measured as the distance from the center of the tokamak to the tip of the exposed material. Once installed the samples were heated above their respective melting points and allowed to degas until the pressure levels inside the tokamak vessel reached their nominal values. Pure Sn samples were heated to 250 °C while the Li–Sn alloy samples were heated to 385 °C. Afterwards the samples were irradiated under deuterium plasmas either in the liquid state, at the previously stated temperatures, or in solid state, at 25 °C. This allowed the comparison between induced effects caused by solid and liquid exposures. After being exposed to the plasma the samples were allowed to solidify and then removed from the tokamak to open air conditions and quickly transferred to ion beam facilities. The reason why deuterium plasmas were used to perform this retention study has to do with its rare occurrence in the atmosphere and consequently any detected quantity can be related directly to this experiment and not contamination.

Samples were analyzed less than 48 h after the last irradiation discharge at the Laboratory of Accelerators and Radiation Technologies using two different ion beam techniques. The quantification of deuterium (D) and lithium (Li) was performed via Nuclear Reaction Analysis (NRA) making use of 1.2 MeV ^{3}He$^+$ beams at a scattering
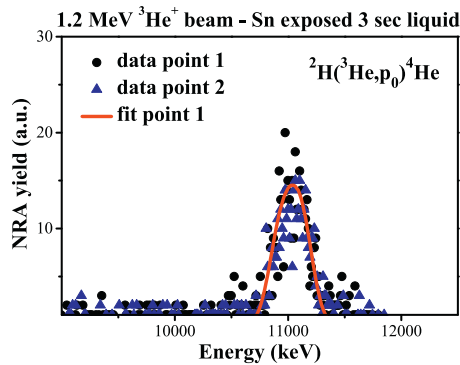
Fig. 2. Nuclear reaction analysis spectrum of a pure Sn sample exposed in liquid state. The NRA spectrum is shown for two different positions (black dots and blue triangles) and the fit (red line) for the first position is shown. (For interpretation of the references to color in this figure legend, the reader is referred to the web version of this article.)

Fig. 3. Nuclear reaction analysis spectrum of a pure Sn sample exposed in solid state. The NRA spectrum is shown for two different positions (black dots and blue triangles) and the fit (red line) for the first position is shown. (For interpretation of the references to color in this figure legend, the reader is referred to the web version of this article.)
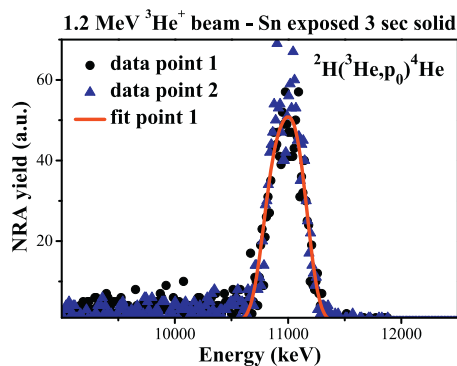

Fig. 4. Nuclear reaction analysis spectrum of a Li–Sn alloy sample exposed in liquid state. The NRA spectrum is shown for two different positions (black dots and blue triangles) and the fit (red line) for the first position is shown. (For interpretation of the references to color in this figure legend, the reader is referred to the web version of this article.)

Fig. 5. Nuclear reaction analysis spectrum of a Li–Sn alloy sample exposed in solid state. The NRA spectrum is shown for two different positions (black dots and blue triangles) and the fit (red line) for the first position is shown. (For interpretation of the references to color in this figure legend, the reader is referred to the web version of this article.)

angle of 140°. A Mylar foil with a thickness of 700 μm was placed in front of the NRA detector in order to decelerate the protons emitted from the $D(^3He,p)^4He$, $^7Li(^3He,p)^9Be$ and $^6Li(^3He,p)^8Be$ nuclear reactions and to avoid the collection of ^4He ions. A collimator located at the entrance of the target chamber assures the incidence of ion beams with a diameter of 1 mm. As it can be seen in Fig. 1 the surface of the sample is rough and therefore it was deemed relevant to analyze each sample on different points in order to assure homogeneity of the exposure. Moreover, carbon (C), oxygen (O) and tin (Sn) depth profiles were evaluated by Rutherford Backscattering (RBS) by using 2.2 MeV incident H^+ ion beams, being the RBS detector located at a scattering angle of 165°. Data analysis was carried out with the IBA Data-Furnace (NDF) code [13,14] and aided with SRIM code [15] simulations.

3. Results and discussion

The NRA spectra and the corresponding best fit lines for all the samples are shown in Figs. 2–5.

Each figure shows two different NRA spectra gathered in two different locations to assure homogeneity of the exposition and of the sample (in the case of the Li–Sn samples) followed by the fit of each spectrum from which the deuterium intake is inferred. The value of the retention measured in absolute by the NRA technique and consequent fit by the NDF software is shown for all samples in Table 1. In previous works the observation of deuterium in the Li–Sn samples was very difficult however taking advantage of longer beam time it was possible to quantify the quantity of deuterium in
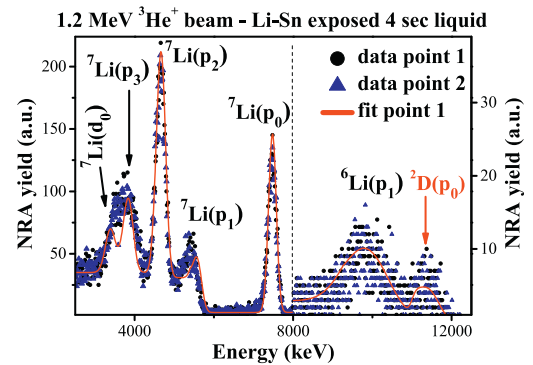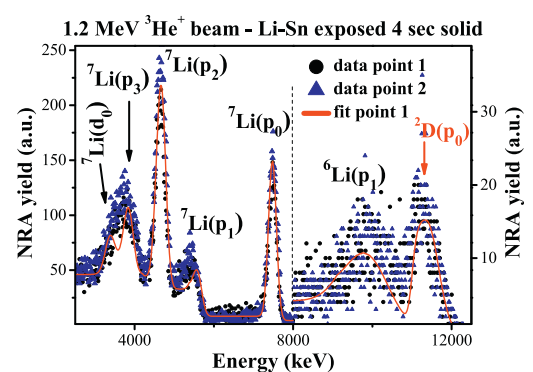
Table 1
Deuterium content in the samples exposed in ISTTOK determined by NRA. The at.% are evaluated for a pure Sn matrix.

Sample	Pos.	D retained (at./cm^2)	D retained (at.%)	Error (%)
Sn solid	1	11.70×10^{15}	0.30	2.6
	2	12.92×10^{15}	0.34	2.5
Sn liquid	1	3.42×10^{15}	0.09	4.5
	2	3.20×10^{15}	0.08	4.7
Li–Sn solid	1	9.92×10^{15}	0.062	3.2
	2	9.59×10^{15}	0.060	3.4
Li–Sn liquid	1	2.70×10^{15}	0.018	7.8
	2	2.85×10^{15}	0.019	7.1

all present samples. Using the cross-sectional data for the interaction of a ^3He beam with 1.2 MeV energy with a deuterium target it is possible to recover the absolute quantity of deuterium retained in the sample without the need to use a reference sample.

The ion flux at the edge of the tokamak was monitored regularly using Langmuir probe data during these discharges. A set of probes in ion saturation was kept at r/a = 0.8, the same radial position where all the samples were exposed. However, this array is installed in a port which is separated from the manipulator 30° in the toroidal direction and 45° in the poloidal direction. The mean value of this quantity was observed to be $\Gamma = 4 \times 10^{22} \pm 0.8 \times 10^{22}$ ion/m^{2}s, where the error is mainly ascribed to the shot to shot reproducibility. We take this quantity as constant throughout all discharges and thus making the particle fluence a function of exposure time.

Table 2

Deuterium content in the samples expressed as retained fraction. The total ion flux is calculated with the total exposition time and retained particles are taken from the average of the two points in Table 1.

$\frac{D_{retained}}{D_{incident}}$	Sn	Li–Sn
Liquid	$(2.76 \pm 0.56) \times 10^{-4}$	$(1.73 \pm 0.36) \times 10^{-4}$
Solid	$(1.03 \pm 0.21) \times 10^{-3}$	$(6.10 \pm 1.23) \times 10^{-4}$

The Sn samples we exposed to 3 s of plasma while the Li–Sn samples were exposed to 4 s. With this we can have the total amount of deuterium impinging on a sample, $D_{incident} = \Gamma \times \Delta t$, and together with the results presented in Table 1 we can define retained fraction as $D_{retained}/D_{incident}$. These fractions, using the average for the two positions, are shown in Table 2. In the balance of deuterium flux to the sample only the ion fraction is accounted and the neutral particle flux is neglected, particularly during the switching of the ISTTOK plasmas. This is a known underestimation however this would further reduce the presented ratios.

From the proton yields observed in the spectra of the Li–Sn samples, shown in Figs. 4 and 5, we evaluate an energy resolution for the present NRA analysis of 120 keV. The corresponding medium values for the depth resolution in metric units are of ≈ 250 nm and ≈ 300 nm for a pure Sn matrix and the Li–Sn alloy, respectively, as given by SRIM [15]. The analysis of the NRA yield led to depth ranges for the retained D amount close to 1 μm in pure Sn and 3.5 μm in Li–Sn. Both these values are lower than those predicted by SRIM code [15] for a $^3He^+$ ion beam impinging either material. Since penetration depth of the NRA beam is higher than of deuterium, the analysis suggests the presence of surface layer where deuterium is retained and negligible amounts should be present at deeper depths. This corroborates the speculated behaviors for this alloy where lithium plays a preferential role in the interaction with the plasma and in particular in fuel retention. However the retention is much lower than the recorded one for pure lithium [16] or for similar alloys [17]. Complementary RBS measurements were made on the samples showing the presence of common airborne contaminants in the alloy's surface such as carbon (≈ 15 at.%) and oxygen (≈ 30 at.%), along superficial layers thinner than 1 μm. The C and O contents strongly decrease with depth. The presence of these elements will contribute to a penetration depth increase of the probing beam. However, the results regarding retention and location would remain mostly unchanged.

Comparing the results for both materials reveals that the retention is lower by almost a factor of 4 and 3, for Sn and Li–Sn respectively, in the case where samples are kept in liquid phase. Since mobility and surface recombination of D in liquid metals are both enhanced at higher temperatures [1], it is not straight forward to discriminate between a diffusion and recombination limited process for the main mechanism behind the present observations. Thus, for pure Li, there are contradictory results in this respect. While Fukada et al. [18] found activation energies for the diffusion of H of 1.6 eV, Moriyama et al. [19] and, very recently, Bi et al. [20] deduced a surface recombination limited mechanisms, with an activation energy of 0.5 eV, from their studies. No data of hydrogen diffusivity in liquid tin have been found, but the results of Sacris and Parlee [21] indicate a very high value for this parameter, on the order of 1 cm^2 s^{-1}, the highest one for the metals addressed in the study (nickel, copper, silver and tin). Assuming that surface recombination is the limiting mechanism for D release, an activation energy of 0.05 eV for the recombination constant of D in Li–Sn is deduced from the data (only two points), i.e, a value 10 lower than that published for liquid lithium surfaces [22]. The same analysis for liquid tin yields an activation energy of 0.06 eV.

It should be pointed out however that surface contamination by O and C, observed by RBS, could have an effect as diffusion barrier thus casting some shadow into the simplified picture here described.

Whatever the mechanism could be, all the obtained retention ratios are all bellow 0.1 at.%. This means that for this particular property these materials are similar to that reported for tungsten [23–25] and outperforms carbon [26]. By itself this suggest that all studied case make good candidates for a PFC.

In fact a comparison between pure Sn and Li–Sn shows that for each state the later roughly half the retention ratio of the former. Although this would seem to indicate that Li–Sn would make a better PFC material, the authors must alert that, being and alloy, the utilization of this material may suffer from stability issues when exposed to a plasma for long times. Since Li is preferentially sputtered/evaporated from the Li–Sn surface, its redeposition on a hot divertor target may change the local stoichiometry of the alloy and therefore its retention properties. More work in this direction is still needed.

The radial impurity content across the plasma column of IST-TOK characterized by visible spectroscopic measurements is envisioned.

4. Summary

The experimental setup and relative experimental procedure for the exposure of tin and lithium–tin alloy samples is described in the present work.

Samples of Sn and Li–Sn were exposed at ISTTOK to deuterium plasmas for comparable total integrated exposure times ($\Gamma^{D+} = 1 - 7 \times 10^{22}/m^2s$; $T_i = 30 - 40$ eV). The samples were irradiated in liquid and solid states (at 250 °C for the pure tin and 385 °C for the alloy for the liquid states). The observation of deuterium retention on the samples was tested with nuclear reaction analysis (NRA) technique. Deuterium retention was observed and quantified in all samples.

References

[1] R. Majeski, R. Kaita, M. Boaz, et al., Testing of liquid lithium limiters in CDX-U, Fus. Eng. Des. 72 (13) (2004) 121–132. Special Issue on Innovative High-Power Density Concepts for Fusion Plasma Chambers.

[2] R. Gomes, H. Fernandes, C. Silva, et al., Interaction of a liquid gallium jet with the tokamak ISTTOK edge plasma, Fus. Eng. Des. 83 (1) (2008) 102–111.

[3] G.G. van Eden, T.W. Morgan, D.U.B. Aussems, et al., Self-regulated plasma heat flux mitigation due to liquid sn vapor shielding, Phys. Rev. Lett. 116 (2016) 135002.

[4] J. Allain, D. Ruzic, M. Hendricks, D, He and Li sputtering of liquid eutectic SnLi, J. Nuc. Mat. 290293 (2001) 33–37. 14th Int. Conf. on Plasma-Surface Interactions in Controlled Fusion Devices.

[5] F.L. Tabarés, Present status of liquid metal research for a fusion reactor, Plasma Phys. Controlled Fusion 58 (1) (2016) 014014.

[6] G. Mazzitelli, M. Apicella, G. Apruzzese, et al., Experiments on FTU with an actively water cooled liquid lithium limiter, J. Nuc. Mat. 463 (2015) 1152–1155. Proceedings of the 21st International Conference on Plasma-Surface Interactions in Controlled Fusion Devices Kanazawa, Japan May 26–30, 2014.

[7] R. Gomes, R. Mateus, E. Alves, et al., Hydrogen retention in gallium samples exposed to ISTTOK plasmas, Fus. Eng. Des. 86 (911) (2011) 2458–2461. Proceedings of the 26th Symposium of Fusion Technology (SOFT-26).

[8] H. Fernandes, C. Varandas, J. Cabral, H. Figueiredo, R. Galvão, Engineering aspects of the ISTTOK operation in a multicycle alternating flat-top plasma current regime, Fus. Eng. Des. 43 (1) (1998) 101–113.

[9] I.S. Carvalho, P. Duarte, H. Fernandes, et al., Real-time control for long ohmic alternate current discharges, Fus. Eng. Des. 89 (5) (2014) 576–581. Proceedings of the 9th IAEA Technical Meeting on Control, Data Acquisition, and Remote Participation for Fusion Research.

[10] J.P.S. Loureiro, F.L. Tabarés, H. Fernandes, et al., Behaviour of liquid Li-Sn alloy as plasma facing material on ISTTOK, in: The Procedings to ISLA-4 Conference, 2015. Granada, Sept. 2015 (to appear in Fus. Eng. Des.).

[11] (http://www.mateck.com/). Accessed: 2016-05-10.

[12] I.S. Carvalho, P. Duarte, H. Fernandes, et al., ISTTOK real-time architecture, Fus. Eng. Des. 89 (3) (2014) 195–203. Design and implementation of real-time systems for magnetic confined fusion devices.

[13] N.P. Barradas, C. Jeynes, R.P. Webb, Simulated annealing analysis of rutherford backscattering data, Appl. Phys. Lett. 71 (2) (1997) 291–293.

[14] (https://www-nds.iaea.org/exfor/exfor.html). Accessed: 2016-05-10.

[15] (http://www.srim.org/). Accessed: 2016-05-10.

[16] E. Oyarzabal, A. Martin-Rojo, F. Tabarés, Laboratory experiments of uptake and release of hydrogen isotopes in liquid lithium, J. Nuc. Mat. 463 (2015) 1173–1176. Proceedings of the 21st International Conference on Plasma-Surface Interactions in Controlled Fusion Devices Kanazawa, Japan May 26–30, 2014.

[17] R. Schumacher, A. Weiss, Hydrogen solubility in the liquid alloys lithium-indium, lithium-lead, and lithium-tin, Ber. Bunsenges Phys. Chem. 94 (6) (1990) 684–691.

[18] S. Fukada, M. Kinoshita, K. Kuroki, T. Muroga, Hydrogen diffusion in liquid lithium from 500 °C to 650 °C, J. Nuc. Mat. 346 (23) (2005) 293–297.

[19] H. Moriyama, K. Iwasaki, Y. Ito, Transport of tritium in liquid lithium, J. Nuc. Mat. 191 (1992) 190–193.

[20] H. Bi, Y. Hirooka, J. Yagi, A study on hydrogen transport in liquid metals under steady state plasma bombardment, Plasma Fus. Res. 11 (2405026) (2016).

[21] E.M. Sacris, N.A.D. Parlee, The diffusion of hydrogen in liquid ni, cu, ag, and sn, Met. Trans. 1 (12) (1970) 3377–3382.

[22] M. Baldwin, R. Doerner, R. Causey, S. Luckhardt, R. Conn, Recombination of deuterium atoms on the surface of molten lilid, J. Nuc. Mat. 306 (1) (2002) 15–20.

[23] T. Tanabe, Review of hydrogen retention in tungsten, Phys. Scr 2014 (T159) (2014) 014044.

[24] R.A. Causey, Hydrogen isotope retention and recycling in fusion reactor plasma-facing components, J. Nuc. Mat. 300 (23) (2002) 91–117.

[25] O. Ogorodnikova, J. Roth, M. Mayer, Pre-implantation and pre-annealing effects on deuterium retention in tungsten, J. Nuc. Mat. 373 (13) (2008) 254–258.

[26] A. Haasz, J. Davis, Deuterium retention in doped graphites, J. Nuc. Mat. 232 (2) (1996) 219–225.